

Voter models on weighted networksAndrea Baronchelli,¹ Claudio Castellano,^{2,3} and Romualdo Pastor-Satorras¹¹*Departament de Física i Enginyeria Nuclear, Universitat Politècnica de Catalunya, Campus Nord B4, 08034 Barcelona, Spain*²*Istituto dei Sistemi Complessi (ISC-CNR), Via dei Taurini 19, I-00185 Roma, Italy*³*Dipartimento di Fisica, "Sapienza" Università di Roma, P.le A. Moro 2, I-00185 Roma, Italy*

(Received 10 November 2010; published 29 June 2011)

We study the dynamics of the voter and Moran processes running on top of complex network substrates where each edge has a weight depending on the degree of the nodes it connects. For each elementary dynamical step the first node is chosen at random and the second is selected with probability proportional to the weight of the connecting edge. We present a heterogeneous mean-field approach allowing to identify conservation laws and to calculate exit probabilities along with consensus times. In the specific case when the weight is given by the product of nodes' degree raised to a power θ , we derive a rich phase diagram, with the consensus time exhibiting various scaling laws depending on θ and on the exponent of the degree distribution γ . Numerical simulations give very good agreement for small values of $|\theta|$. An additional analytical treatment (heterogeneous pair approximation) improves the agreement with numerics, but the theoretical understanding of the behavior in the limit of large $|\theta|$ remains an open challenge.

DOI: [10.1103/PhysRevE.83.066117](https://doi.org/10.1103/PhysRevE.83.066117)

PACS number(s): 89.75.Hc, 05.65.+b

I. INTRODUCTION

Many technological, biological, and social networks are intrinsically weighted. Each link has associated an additional variable, called weight, which gauges the intensity or traffic of that connection, and that can exhibit widely varying fluctuations [1–3]. The presence of weights is extremely relevant in some scenarios (e.g., in the case of transport in a network in which weights measure bandwidth or capacity), and it must therefore be taken into account explicitly. Some results have already been produced in this direction, dealing, among other problems, with diffusive processes [4,5], epidemic spreading [6,7], general equilibrium and nonequilibrium phase transitions [8,9], or glassy dynamics [10]. Here we present a detailed investigation of the ordering dynamics of voterlike models on weighted networks [11].

The voter model [12,13] and the Moran process [14] are simple examples of ordering dynamics, which allow to understand how natural systems with an initial disordered configuration are able to achieve order via local pairwise interactions. Both models are described in terms of a collection of individuals, each endowed with a binary variable s_i , taking the values ± 1 . The elementary step consists in randomly choosing a first individual and then (again randomly) one of her nearest neighbors. In the voter model the first individual will *copy* the state of her neighbor. In the Moran process, on the other hand, she will *transmit* her own state to the neighboring node, which will adopt it. In both cases, starting from a disordered initial state, the iteration of the elementary step leads to the growth of correlated domains and, in finite systems, to an absorbing uniform state in which all individuals share the same state (the so-called consensus). In a social science context, the voter model represents thus the simplest model of opinion formation in a population, in which individuals can change their opinion as a function of the state of their nearest neighbors [11]. In the same way, in a biological context, the Moran process represents the elementary example of two species competing (through reproduction and neutral selection) for the same environment [15].

The voter and Moran processes are equivalent on regular lattices and on the complete graph, but if the pattern of connections is given by a complex (unweighted) topology they behave differently, since the order in which interacting individuals are selected becomes relevant [16,17]. Moreover, the time to reach consensus scales with the system size in different ways depending on the degree distribution of the network [18–20]. Considering a weighted topological substrate adds, as we will see, a richer and more complex phenomenology. Additionally, the case of weighted networks allows to model very natural settings. In the context of social sciences, for example, weights can reflect the obvious fact that the opinion of a given individual can be more easily influenced by a close friend rather than by a casual acquaintance. On the other hand, in an evolutionary scenario, weights allow to gauge the effects of heterogeneous replacement rates in different species.

On weighted networks, at each time step a vertex i is selected randomly with uniform probability; then one nearest neighbor of i , namely, j , is chosen with a probability proportional to the weight $w_{ij} \geq 0$ of the edge joining i and j . That is, the probability of choosing the neighbor j is

$$P_{ij} = \frac{w_{ij}}{\sum_r w_{ir}}. \quad (1)$$

Vertices i and j are then updated according to the rules of the respective models. With this definition, the models considered represent the natural extension for ordering dynamics on weighted networks (and in particular of the voter model) of the generalized Moran process proposed in Refs. [21] and [22], in which dynamics was defined as a function of a set of arbitrary interaction probabilities P_{ij} . In our case, however, the fact that these interaction probabilities arise from the normalized weights arriving at a vertex imposes some restrictions to the possible values of P_{ij} and yields therefore different outcomes and interpretations. Also, it is worth noting three recent publications [23–25], dealing with related, but not identical, models.

Adopting the heterogeneous mean-field (HMF) approximation [26,27] we will assume that the weight between vertices i and j depends only on the degrees at the edges endpoints, namely, k_i and k_j , and therefore we can write $w_{ij} \equiv g(k_i, k_j) a_{ij}$, where a_{ij} is the adjacency matrix and $g(k, k')$ is a positive definite, symmetric function. The application of HMF theory and the backward Fokker-Planck formalism [18–20] allows us to derive analytical expressions in degree uncorrelated networks for the main relevant quantities (namely, exit probability and consensus time [11]) in a more transparent way than in Refs. [21] and [22]. In order to allow for closed mathematical solutions of the models, we will further specify the function g to be given by the product of two independent functions $g(k, k') = g_s(k)g_s(k')$, an assumption motivated by empirical observations in real weighted networks [1]. Specializing both models to the case of networks with power-law distributed degrees and edge weights given by multiplicative powers the endpoint degrees, $g_s(k) = k^\theta$, a very rich phase diagram is obtained, with several different scaling regions of the consensus time with the network size N . A numerical check of the analytical predictions reveals a good agreement in some regions of the parameters space and noticeable discrepancies in others. In order to gain insights into the observed numerical disagreement, we apply an improved mean-field approach, the heterogeneous pair approximation [28], which turns out to provide better agreement with numerics for small θ but is still not able to solve the problems for large θ . The qualitatively different nature of the dynamics for large θ is briefly discussed and its understanding identified as an intriguing challenge for future work.

II. HETEROGENEOUS MEAN-FIELD THEORY

In this section, we perform a theoretical analysis of the voter and Moran processes on weighted networks within a HMF approximation [26], extending the Fokker-Planck formalism developed for the unweighted case in Refs. [18–20]. Let us consider the models defined by the interaction probability Eq. (1), where the network weights take the form

$$w_{ij} = g(k_i, k_j) a_{ij}. \quad (2)$$

The simplest way to extend the Fokker-Planck approach to weighted networks is to follow the annealed weighted network approximation introduced in Ref. [5]. The key point consists in considering the degree coarse-grained interaction probability $P_w(k \rightarrow k')$, defined as the probability that a vertex of degree k interacts with a nearest-neighbor vertex of degree k' . In unweighted networks, this probability simply takes the form of the conditional probability $P(k'|k)$ that a vertex of degree k is connected to a vertex of degree k' [29]. In networks with weights given by Eq. (2), the interaction probability of the voter and Moran dynamics, Eq. (1), can be coarse grained by performing an appropriate degree average, to yield [5]

$$P_w(k \rightarrow k') = \frac{g(k, k') P(k'|k)}{\sum_q g(k, q) P(q|k)}. \quad (3)$$

The relevant function defining voter and Moran processes is the probability $\Pi(k; s)$ that a spin s at a vertex of degree k flips its value to $-s$ in a microscopic time step [18–20]. This function can be expressed, within the annealed weighted

network approximation, in terms of the density x_k of $+1$ spins in vertices of degree k , taking the form

$$\Pi_V(k; +1) = P(k) x_k \sum_{k'} P_w(k \rightarrow k') (1 - x_{k'}), \quad (4)$$

$$\Pi_V(k; -1) = P(k) (1 - x_k) \sum_{k'} P_w(k \rightarrow k') x_{k'}, \quad (5)$$

for the voter model. The origin of these probabilities is easy to understand [18–20]. For example, Eq. (4) gives the probability of flipping a vertex of degree k in the state $+1$ as the product of the probability $P(k)$ of choosing a vertex of degree k , times the probability x_k that the vertex is in the state $+1$, times the probability k chooses to interact with a neighbor vertex k' , which is in state -1 with probability $1 - x_{k'}$, averaged over all possible neighbor degrees k' . Analogously, the flipping probabilities for the Moran process can be expressed as

$$\Pi_M(k; +1) = \sum_{k'} P(k') (1 - x_{k'}) P_w(k' \rightarrow k) x_k, \quad (6)$$

$$\Pi_M(k; -1) = \sum_{k'} P(k') x_{k'} P_w(k' \rightarrow k) (1 - x_k). \quad (7)$$

Let us now present separately the mean-field analysis for the two models under consideration.

A. Voter model

1. Rate equation, conservation laws, and exit probability

Let us consider the time evolution of the density x_k , which is determined in terms of a rate equation. Following Refs. [5,17–20], this rate equation is shown to take the form

$$\begin{aligned} \dot{x}_k(t) &= \sum_{k'} P_w(k \rightarrow k') x_{k'}(t) - x_k(t) \\ &= \sum_{k'} \frac{g(k, k') P(k'|k)}{\sum_q g(k, q) P(q|k)} x_{k'}(t) - x_k(t), \end{aligned} \quad (8)$$

where in the last expression we have used Eq. (3). The complete expression Eq. (8), valid for any correlation and weight patterns, is quite difficult to deal with. In order to obtain closed analytical expressions, we assume that the underlying network is degree uncorrelated, namely, $P(k'|k) = k' P(k') / \langle k \rangle$ [30], and moreover, that the weights are simple multiplicative functions of the edges' end points, that is, $g(k, k') = g_s(k) g_s(k')$. In this way, Eq. (8) becomes

$$\dot{x}_k(t) = \omega_V(t) - x_k(t), \quad (9)$$

where we have defined

$$\omega_V(t) = \sum_{k'} \frac{k' g_s(k') P(k')}{\langle k g_s(k) \rangle} x_{k'}(t), \quad (10)$$

and $\langle f(k) \rangle \equiv \sum_k P(k) f(k)$.

It is easy to see that the total density of $+1$ spins, $x = \sum_k P(k) x_k$, is not a conserved quantity, $\dot{x} = -x + \omega_V$. The quantity ω_V , however, is conserved, $\dot{\omega}_V(t) = 0$, as we can see by inserting Eq. (9) into the time derivative of $\omega_V(t)$. Finally, the steady-state condition of Eq. (9), $\dot{x}_k = 0$, implies $x_k = \omega_V$.

As for the usual voter model [18,20] the conservation law allows the immediate determination of the exit (or

“fixation”) probability E , i.e., the probability that the final state corresponds to all spins in the state $+1$. In the final state with all $+1$ spins we have $\omega_V = 1$, while $\omega_V = 0$ is the other possible final state (all -1 spins). Conservation of ω_V implies then $\omega_V = E \cdot 1 + [1 - E] \cdot 0$, hence

$$E = \omega_V. \quad (11)$$

Starting from an homogeneous initial condition, with a density x of randomly chosen vertices in the state $+1$, we obtain, since $\omega_V = x$, $E_h(x) = x$ as in the standard voter model [11]. On the other hand, with initial conditions consistent of a single $+1$ spin in a vertex of degree k , we have $E_1(k) = kg_s(k)/[N\langle kg_s(k) \rangle]$.

2. Consensus time

The backward Fokker-Planck formalism [31] can be applied to obtain expressions for the consensus time $T_N(x)$, as a function of the initial density x of $+1$ spins and the system size N . However, following Refs. [17–20], it is simpler to apply a one-step calculation and use the recursion relation [18–20]

$$T_N(\{x_k\}) = \sum_s \sum_k \Pi_V(k; s) [T_N(x_k - s \Delta_k) + \Delta t] + Q(\{x_k\}) [T_N(\{x_k\}) + \Delta t], \quad (12)$$

where $Q = 1 - \sum_s \sum_k \Pi_V(k; s)$ is the probability than no spin flip takes place, $\Delta t = 1/N$, and $\Delta_k = 1/[NP(k)]$ is the change in x_k when a spin flips in a vertex of degree k . Rearranging the terms in Eq. (12), and expanding to second order in Δ_k , we obtain

$$\frac{1}{2N} \sum_k \frac{x_k + \omega_V - 2x_k \omega_V}{P(k)} \frac{\partial^2 T_N}{\partial x_k^2} + \sum_k (x_k - \omega_V) \frac{\partial T_N}{\partial x_k} = -1. \quad (13)$$

Equation (13) is simplified by observing that the ordering dynamics of the voter model is separated in two well distinct temporal regimes [18,32]. Over a short time the different densities x_k all converge from their initial value to the common value at the steady state $x_k = \omega_V$. For infinite-size systems, this state survives forever. For finite size N , the system enters instead a different regime, where the dynamics of densities x_k is enslaved by the fluctuations of ω_V , which performs a slow diffusion until it hits the absorbing values 0 or 1. The consensus time is dominated by this second regime. This allows to apply the steady-state condition which cancels the drift term in Eq. (13). Taking as relevant quantity the conserved weighted magnetization ω_V , we obtain [18,20]

$$\frac{1}{N} \omega_V (1 - \omega_V) \frac{\langle k^2 g_s(k)^2 \rangle}{\langle kg_s(k) \rangle^2} \frac{\partial^2 T_N}{\partial \omega_V^2} = -1. \quad (14)$$

The integration of this equation leads to

$$T_N(\omega_V) = -N \frac{\langle kg_s(k) \rangle^2}{\langle k^2 g_s(k)^2 \rangle} [\omega_V \ln \omega_V + (1 - \omega_V) \ln(1 - \omega_V)].$$

Thus, the ordering time starting from homogeneous initial conditions $x_k = \omega_V = 1/2$ is

$$T_N(x = 1/2) = N(\ln 2) \frac{\langle kg_s(k) \rangle^2}{\langle k^2 g_s(k)^2 \rangle}. \quad (15)$$

B. Moran process

1. Rate equation, conservation laws, and exit probability

The derivation of the rate equation for the density x_k in the Moran process follows the same steps as in the voter model, taking the form

$$\begin{aligned} \dot{x}_k(t) &= \frac{1}{P(k)} \sum_{k'} P(k') P_w(k' \rightarrow k) [x_k(t) - x_{k'}(t)] \\ &= k \sum_{k'} \frac{P(k'|k)}{k'} \frac{g(k'|k)}{\sum_q g(k',q) P(q|k')} [x_k(t) - x_{k'}(t)], \end{aligned}$$

where in the last step we used the degree detailed balance condition $k P(k) P(k'|k) = k' P(k') P(k|k')$ [33]. Assuming again a degree uncorrelated network, and multiplicative weights, we are led to

$$\dot{x}_k(t) = \frac{kg_s(k)}{\langle kg_s(k) \rangle} [x_k(t) - x(t)]. \quad (16)$$

Again, the total density of $+1$ spins, $x = \sum_k P(k) x_k$ is not conserved, while instead the quantity

$$\omega_M = \frac{1}{\langle [kg_s(k)]^{-1} \rangle} \sum_k \frac{P(k)}{kg_s(k)} x_k \quad (17)$$

is conserved, $\dot{\omega}_M = 0$. Finally, from the steady-state condition $\dot{x}_k = 0$, we obtain $x_k = x$. From the conservation of ω_M the exit probability is immediately derived as

$$E = \omega_M. \quad (18)$$

Homogeneous initial conditions lead again to $E_h(x) = x$, while a single $+1$ spin in a vertex of degree k leads to

$$E_1(k) = \frac{1}{kg_s(k)} \frac{1}{N \langle [kg_s(k)]^{-1} \rangle}. \quad (19)$$

It is interesting to note that in the conserved quantity of the voter model ω_V , each density x_k is weighted with the product $kg_s(k)$ [Eq. (10)], while in the correspondent ω_M for the Moran process the weight is precisely the inverse, namely, $[kg_s(k)]^{-1}$ [Eq. (17)]. As noted in the case of unweighted networks [20], intuitively this can be ascribed to the fact that in the voter model it is the first selected node that may change its state, while in the Moran process it is the second one. Thus in the voter model small-degree nodes change their state more often than high-degree nodes, and weighting them with the probability of being chosen $[kg_s(k)]$ compensates this disparity, leading to the conserved quantity ω_V . Vice versa in the Moran process low-degree nodes change their state less often than high-degree nodes, and the inverse weighting balances this difference [20].

2. Consensus time

Following the same steps presented for the voter model, and performing the appropriate expansion to second order in Δ_k , we obtain the equation

$$\begin{aligned} \sum_k \frac{kg_s(k)}{\langle kg_s(k) \rangle} (x_k - x) \frac{\partial T_N}{\partial x_k} \\ + \frac{1}{2N} \sum_k \frac{kg_s(k)}{\langle kg_s(k) \rangle} \frac{x_k + x - 2x_k x}{P(k)} \frac{\partial^2 T_N}{\partial x_k^2} = -1. \end{aligned}$$

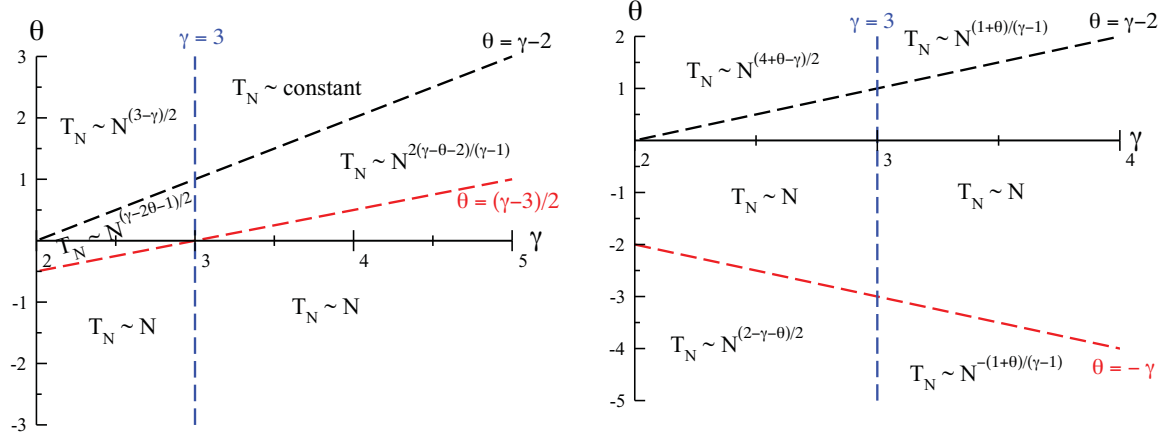


FIG. 1. (Color online) Phase diagram of the voter model (left-hand side) and Moran process (right-hand side) on weighted scale-free networks.

The steady-state condition $x_k = x$ leads to the cancellation of the drift term. The diffusion term is simplified by changing variables with the conserved quantity ω_M , leading to the equation

$$\frac{1}{N} \frac{1}{\langle [kg_s(k)]^{-1} \rangle} \frac{\omega_M(1-\omega_M)}{\langle kg_s(k) \rangle} \frac{\partial^2 T_N}{\partial \omega_M^2} = -1, \quad (20)$$

where we have used the fact that, in the steady state, $x = \omega_M$. The solution of equation for the consensus time leads now to

$$T_N(\omega_M) = -N \langle kg_s(k) \rangle \langle [kg_s(k)]^{-1} \rangle \times [\omega_M \ln(\omega_M) + (1-\omega_M) \ln(1-\omega_M)]. \quad (21)$$

Thus, starting from homogeneous initial conditions $x_k = x = \omega_M = 1/2$, we have

$$T_N(x = 1/2) = N(\ln 2) \langle kg_s(k) \rangle \langle [kg_s(k)]^{-1} \rangle. \quad (22)$$

III. NETWORKS WITH POWER-LAW DEGREE DISTRIBUTION AND WEIGHT STRENGTHS

The actual behavior of the exit probability and the consensus time depends, in view of the previous calculations, on the topological properties of the network under consideration, as well as on the strength of the weights, as given by the function $g_s(k)$. In this section we consider explicitly these dependencies for the particular case of networks with a power-law degree distribution form $P(k) \sim k^{-\gamma}$, and a weight strength scaling also as a power of the degree $g_s(k) = k^\theta$. This last selection is reasonable in view of the weight patterns empirically observed in real networks [1]. Let us focus on the consensus time with homogeneous ($x = 0.5$) initial conditions for the two models considered.

In the case of the voter model, the ordering time with homogeneous initial conditions and weights scaling as a power of k takes the form

$$T_N(1/2) = N \ln(2) \frac{\langle k^{1+\theta} \rangle^2}{\langle k^{2+2\theta} \rangle}. \quad (23)$$

From this expression, we can obtain different scalings with the network size N , depending on the characteristic exponents γ

and θ ; we consider only $\gamma > 2$. Using the fact that $\langle k^a \rangle \sim \text{const}$ for $a < \gamma - 1$ and $\langle k^a \rangle \sim k_c^{a+1-\gamma}$ for $a > \gamma - 1$, where k_c is the upper network cutoff, and, in view of the comparison with numerical results for the uncorrelated configuration model (UCM) [34], considering the scaling $k_c \sim N^{1/2}$ for $\gamma < 3$ and $k_c \sim N^{1/(\gamma-1)}$ for $\gamma > 3$ [35], we obtain the following scaling for consensus the time:

$$T_N(1/2) \sim \begin{cases} N^{(3-\gamma)/2}, & \theta > \gamma - 2, \gamma < 3, \\ \text{const}, & \theta > \gamma - 2, \gamma > 3, \\ N^{(\gamma-2\theta-1)/2}, & \gamma - 2 > \theta > (\gamma-3)/2, \gamma < 3, \\ N^{2(\gamma-\theta-2)/(\gamma-1)}, & \gamma - 2 > \theta > (\gamma-3)/2, \gamma > 3, \\ N, & \theta < (\gamma-3)/2. \end{cases} \quad (24)$$

In Fig. 1 (left-hand side) we represent graphically the different scalings of the consensus time T_N in the (θ, γ) space.

For the Moran process, the ordering time scales with the network size through the expression

$$T_N(1/2) = N \ln(2) \langle k^{1+\theta} \rangle \langle k^{-1-\theta} \rangle. \quad (25)$$

For $\gamma > 2$, the different possible scalings are as follows:

$$T_N(1/2) \sim \begin{cases} N^{(4+\theta-\gamma)/2}, & \theta > \gamma - 2, \gamma < 3, \\ N^{(1+\theta)/(\gamma-1)}, & \theta > \gamma - 2, \gamma > 3, \\ N, & -\gamma < \theta < \gamma - 2, \\ N^{-(1+\theta)/(\gamma-1)}, & \theta < -\gamma, \gamma > 3, \\ N^{(2-\theta-\gamma)/2}, & \theta < -\gamma, \gamma < 3. \end{cases} \quad (26)$$

Figure 1 (right-hand side) depicts the different regimes associated to the behavior of T_N in the (θ, γ) space.

Some comments are now in order. First we notice that all relevant quantities are in fact functions of the combination $k^{\theta+1}$. This implies that for $\theta = -1$ both voter and Moran dynamics are predicted to give the same results at the mean-field level, independently of the degree distribution. In fact, $\theta = -1$ implies that both interacting vertices are extracted completely at random (independently of their degree) so that the asymmetry distinguishing the voter model from the Moran process vanishes. For other values of θ , on the other hand, the effect of weights appears to be completely different for

the two dynamics. For the voter model, positive values of θ tend to reduce the consensus time, while $\theta < 0$ leads to increased T_N , i.e., the dynamics becomes slower. In any case the consensus time is at most proportional to the system size N : The dynamics is always relatively fast. Interestingly, the HMF analysis predicts the presence of a region ($\theta > \gamma - 2$ and $\gamma > 3$) for which the consensus time is constant, i.e., the dynamics undergoes an instantaneous ordering process, in contrast with what happens in other regions, in which ordered regions of opposite states can coexist for very long times, reaching consensus only in finite systems and through a large stochastic fluctuation [36]. As it will be shown below, this is true only on annealed networks in which the quenched disorder imposed by the actual connections in the network is not considered. Numerical simulations performed on quenched graphs give different results.

For the Moran process, on the other hand, $T \sim N$ represents a lower bound for the scaling of the consensus time: The dynamics is always rather slow, with an exponent larger than 1 for all (γ, θ) . Remarkably, the scaling of T_N turns out to depend symmetrically on $|\theta + 1|$: A large positive or a large negative value of $\theta + 1$ are equally effective in slowing down the ordering process.

IV. COMPARISON WITH NUMERICAL SIMULATIONS

A. Algorithms

In order to check the analytical predictions for the voter model and Moran process, we have performed numerical simulations of both models on uncorrelated networks generated using the UCM [34]. The networks have a degree exponent γ , a minimum degree $k_m = 4$, and a maximum degree smaller than or equal to \sqrt{N} , preventing the generation of correlations for $\gamma < 3$ [35]. A weight strength $g_s(k) = k^\theta$ is imposed by selecting a nearest neighbor j of a vertex i with probability

$$P_{ij} = \frac{k_j^\theta}{\sum_{v \in \mathcal{V}(i)} k_v^\theta}, \tag{27}$$

where $\mathcal{V}(i)$ is the set of nearest neighbors of i .

Moreover, since HMF equations describe in an exact way dynamics taking place on annealed networks [5], we have simulated the voter model and the Moran process also on such structures, in order to provide a benchmark of our analytical results. In annealed networks, in fact, all links are rewired at each microscopic time step, so that no dynamical correlation can build up, and the absence of correlations assumed by mean-field approaches is actually implemented. In weighted networks, the probability that a vertex of degree k interacts with a vertex of degree k' is given by

$$P_w(k \rightarrow k') = \frac{k' g_s(k') P(k')}{\langle k g_s(k) \rangle} = \frac{k'^{1+\theta} P(k')}{\langle k^{1+\theta} \rangle}, \tag{28}$$

where in the last equality we have assumed again that $g_s(k) = k^\theta$. An annealed weighted network is thus implemented by choosing as neighbor of any given vertex another vertex of degree k , randomly chosen in the network with probability proportional to $k^{1+\theta}$ [5]. In a quenched network, on the other hand, the neighbors of the first node are of course fixed and the choice is restricted to them.

B. Exit probability

While for homogeneous initial conditions both the voter model and Moran process lead to an exit probability equal to the standard voter model, i.e., $E(x) = x$, invasion initial conditions starting from a single +1 spin in a vertex of degree k lead to exit probabilities that depend explicitly on the initial degree considered. In particular, we find

$$E_1^{\text{voter}}(k) \sim k^{1+\theta}, \quad E_1^{\text{Moran}}(k) \sim k^{-(1+\theta)}. \tag{29}$$

While for the voter model a single +1 vertex has better chances to invade the system if it starts from a high degree vertex, for the Moran process the situation is precisely the opposite, a single +1 spin being favored when initially located in the vertices of smallest degree. This kind of behavior is actually to be expected from the very definition of the models, and has been already reported in unweighted networks [20]. In fact, a high degree is beneficial in the voter model since it corresponds to a larger probability of being chosen as a partner by a neighbor in search for an opinion to copy, while in the Moran process having many neighbors implies a larger probability to be invaded by the opinion at one of them. In Fig. 2 we plot the values of the exit probability $E_1(k)$ computed from numerical simulations. The results fit quite nicely the mean-field predictions in Eq. (29): The larger the weight intensity, the stronger the impact of high- and low-degree vertices in the voter and Moran processes, respectively.

C. Consensus time

In Fig. 3 we check the validity of the scaling behaviors predicted by the HMF treatment and sketched in Fig. 1. In this figure, we plot the scaling of the consensus time T_N as a function of N , for different points in the six regions in which the respective phase diagrams are divided, compared with the corresponding theoretical mean-field predictions.

Figure 3 shows that, overall, the agreement between the scaling predicted by theory and numerical data in annealed networks is, as expected, very good. With respect to the results for quenched networks, the agreement between HMF theory and simulations is in general restricted to small absolute values of θ , as reported for other dynamical processes [5]. In order

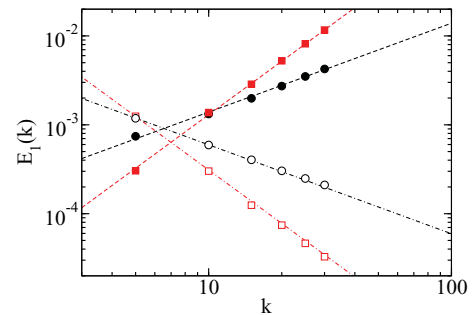


FIG. 2. (Color online) Exit probability $E_1(k)$ starting from a single +1 spin in a vertex of degree k , for the voter model (filled symbols) and the Moran process (open symbols). Dashed lines represent the expected theoretical scaling with k , circles refer to the case $\theta = 0$ and squares to $\theta = 1$. Data from quenched networks of size $N = 10^3$ with $\gamma = 2.5$ (voter model) and $\gamma = 2.2$ (Moran process).

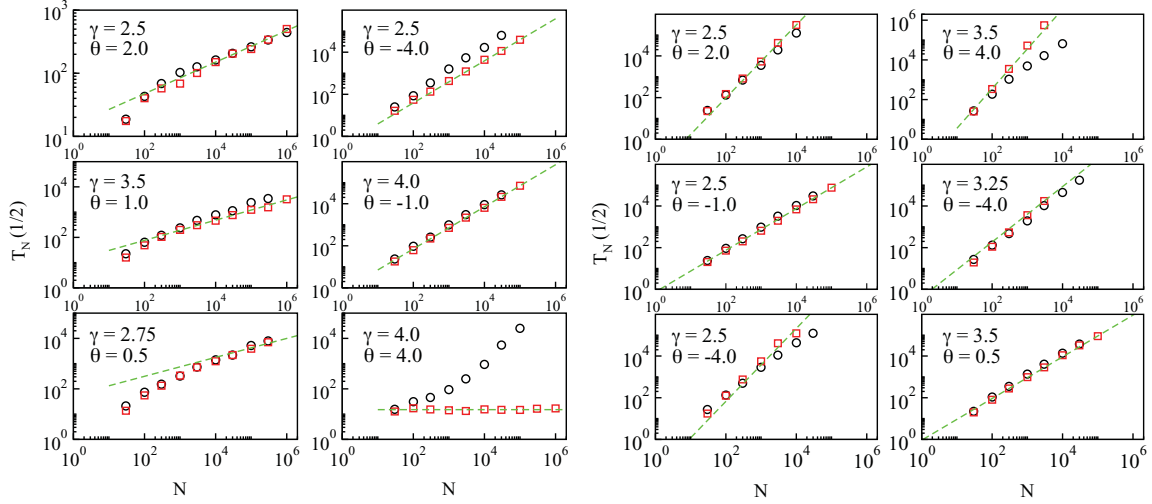


FIG. 3. (Color online) Scaling with N for the voter model (left-hand side) and Moran process (right-hand side) on scale-free weighted networks in different regions of the corresponding phase diagrams, Fig. 1. Squares represent data from simulations run on annealed networks, while circles concern quenched graphs. Dashed lines represent the theoretical scaling predicted by HMF theory.

to set better limits to the validity of the HMF approximation, in Fig. 4 we report the numerical values of the consensus time obtained from simulations in quenched networks of fixed size $N = 3 \times 10^3$ in slices of the phase diagrams in Fig. 1 performed at two constant values of γ , one larger and one smaller than 3, and varying θ . These numerical values are compared with numerical evaluations of the theoretical predictions in Eqs. (23) and (25). From Fig. 4 we observe that the HMF approximation yields reasonably correct results except for large values of θ (for $\gamma > 3$) or large values of $-\theta$ (for $\gamma < 3$). When these errors occur, consensus time is underestimated by HMF for the voter model, while it is overestimated for the Moran process. At the present stage we are not able to predict *a priori* when the theoretical results fail to describe the behavior of the dynamics taking place on quenched networks, but the numerical evidence suggests that the theory works well for values of $|\theta|$ of the order of those observed in real networks [1].

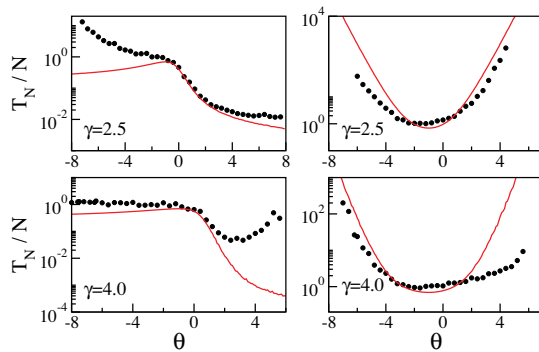


FIG. 4. (Color online) Consensus time for the voter model (left-hand side) and Moran process (right-hand side) in slices of the phase diagrams at two fixed values of γ and varying θ , compared with the corresponding HMF predictions, Eqs. (23) and (25), respectively (full lines). Results from simulations performed on quenched networks of size $N = 3 \times 10^3$.

V. HETEROGENEOUS PAIR APPROXIMATION

There are several possible assumptions in the HMF treatment which could fail when the approach breaks down. One is the assumption that the time to reach consensus is dominated by the diffusive wandering of the quasisteady state, which is much larger than the time to reach such a state. More important is, however, the possibility that the very first hypothesis at the core of mean-field theory, namely, that the dynamics of the system can be fully described in terms of the densities x_k , breaks down [28,32]. This assumption can be violated at several different levels. A mild violation occurs when the probability of a node to be in a +1 state is correlated with the state of its nearest neighbors. In order to ascertain this possibility, it is useful to consider the quantity ρ_k , defined as the probability that an edge connected to a node of degree k and selected for the dynamics is active, i.e., it connects nodes in a different state. Focusing on the case of the voter model, HMF theory, which explicitly assumes the lack of dynamical correlations between the vertices at the ends of any edge, predicts that this quantity should be equal to

$$\begin{aligned} \rho_k &= \sum_{k'} P_w(k \rightarrow k') [x_k(1 - x_{k'}) + (1 - x_k)x_{k'}] \\ &= x_k(1 - \omega_V) + (1 - x_k)\omega_V \end{aligned} \quad (30)$$

and hence, for initial homogeneous conditions $x_k = x = \omega_V = 1/2$, we should have in the stationary state $\rho_k^S = 2x(1 - x) = 1/2$.

Figure 5 shows that, for a case where the mean field is not accurate, this assumption is not correct in two respects: First, the value of ρ_k is lower than 1/2 (dashed line), indicating that, in fact, correlations build up in the system. Second, ρ_k depends on k , implying that those correlations depend, moreover, on the degree of the nodes.

In order to take into account these degree-dependent dynamical correlations, one needs to consider, as a relevant dynamical variable, the probability $\rho_{k,k'}$ that an edge connecting a node of degree k with another node of degree k' is active, i.e.,

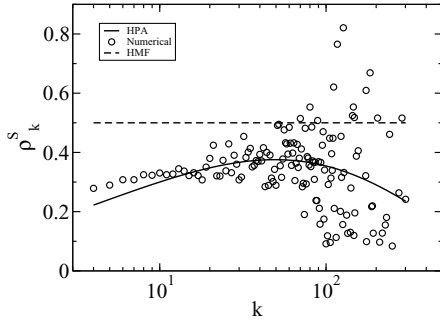


FIG. 5. Probability ρ_k^S that an edge connected to a node of degree k and selected for the dynamics is active as a function of k , in the quasisteady state for $x = 1/2$. The solid line is the result of the heterogeneous pair approximation, while symbols are results of numerical simulations. Binning has deliberately been avoided to show the large variability of numerical results for larger degrees. Data from voter dynamics on quenched networks of size $N = 10^5$, with $\gamma = 3.25$ and $\theta = 1.5$.

the two nodes are in a different state. This approach, termed the heterogeneous pair approximation (HPA), has been introduced and applied to voter models on unweighted networks in Ref. [28]. To determine the equation of motion of the quantity $\rho_{k,k'}$ in the voter model, we observe that this quantity is modified if the flipping node has degree k and one of its neighbors has degree k' (or vice versa). Let us assume that the flipping (first selected) node has degree k and call k'' the degree of the copied (second selected) node. It is useful to consider separately the two cases where $k'' \neq k'$ or $k'' = k'$.

In the first case the variation $\Delta\rho_{k,k'}$ for a single dynamical step (occurring over a time $\Delta t = 1/N$) is determined as follows: The probability that a node in state s and degree k flips is given by the probability $P(k)$ that the first node selected has degree k times the probability $\sigma(s)$ that it is in state s , times the probability $P_w(k \rightarrow k'')$ that the second has degree k'' multiplied by the probability $\rho_{k,k''}/[2\sigma(s)]$ that the link connecting the two is active. One has then to multiply this quantity by the associated variation of the fraction of active links between k and k' . Among the $k-1$ other links of the flipping node, the number of those connecting to a node of degree k' will be j distributed according to a binomial $R(j, k-1)$ with probability of the single event equal to $P(k'|k)$. In their turn, only n out of these j links will be active, with n binomially distributed $[B(n, j)]$ with single event probability $\rho_{k,k'}/[2\sigma(s)]$. Finally one has to multiply by the variation of $\rho_{k,k'}$ when n out of j links go from active to inactive as a consequence of the flipping of the node in k . This is given by the variation of the number of active links $[(j-n) - n]$ divided the total number of links between nodes of degree k and k' , namely, $NkP(k)P(k'|k)$. One has then to sum over $k'' \neq k'$, s , j and n , obtaining

$$\begin{aligned} \Delta\rho_{k,k'} &= P(k) \sum_s \sigma(s) \sum_{k'' \neq k'} P_w(k \rightarrow k'') \frac{\rho_{k,k''}}{2\sigma(s)} \\ &\times \sum_{j=0}^{k-1} R(j, k-1) \sum_{n=0}^j B(n, j) \frac{j-2n}{NkP(k)P(k'|k)}. \end{aligned} \quad (31)$$

By performing explicitly the summations [and using $\sum_s 1/\sigma(s) = 4/(1-m^2)$, where $m = 2x - 1$ is the magnetization] the formula becomes

$$\frac{\Delta\rho_{k,k'}}{\Delta t} = \sum_{k'' \neq k'} P_w(k \rightarrow k'') \rho_{k,k''} \frac{(k-1)}{k} \left(1 - \frac{2}{1-m^2} \rho_{k,k'} \right). \quad (32)$$

When $k'' = k'$, the value of $\Delta\rho_{k,k'}$ is similar to Eq. (31) with (obviously) $P_w(k \rightarrow k')$ instead of $P_w(k \rightarrow k'')$, no sum over k'' , and in the numerator of the last factor $j+1 - (n+1) - (n+1) = j-2n-1$, because there are $j+1$ links to nodes of degree k , $n+1$ of which are active in the initial state and inactive in the final. Summing up the two contributions and adding the symmetric terms with k and k' swapped, we get

$$\begin{aligned} \frac{d\rho_{k,k'}}{dt} &= \rho_k \frac{k-1}{k} + \rho_{k'} \frac{k'-1}{k'} \\ &+ -\rho_{k,k'} \left[\frac{P_w(k \rightarrow k')}{P(k'|k)} \frac{1}{k} + \frac{P_w(k' \rightarrow k)}{P(k|k')} \frac{1}{k'} \right] \\ &+ \frac{2\rho_k}{1-m^2} \frac{k-1}{k} + \frac{2\rho_{k'}}{1-m^2} \frac{k'-1}{k'}. \end{aligned} \quad (33)$$

When uncorrelated networks are considered, so that

$$\frac{P_w(k \rightarrow k')}{P(k'|k)} = \frac{\langle k \rangle}{\langle k^{1+\theta} \rangle} k'^{\theta}, \quad (34)$$

we are led to the final equation

$$\begin{aligned} \frac{d\rho_{k,k'}}{dt} &= \rho_k \frac{k-1}{k} + \rho_{k'} \frac{k'-1}{k'} - \rho_{k,k'} \left[\frac{\langle k \rangle}{\langle k^{1+\theta} \rangle} \left(\frac{k^{\theta}}{k} + \frac{k^{\theta}}{k'} \right) \right] \\ &+ \frac{2\rho_k}{1-m^2} \frac{k-1}{k} + \frac{2\rho_{k'}}{1-m^2} \frac{k'-1}{k'}. \end{aligned} \quad (35)$$

where m is the magnetization and, at odds with the case of unweighted networks, the definition of ρ_k is now

$$\rho_k = \sum_{k'} P_w(k \rightarrow k') \rho_{k,k'}. \quad (36)$$

Solving numerically this equation in the stationary state, it is possible to determine ρ_k^S , which turns out to be in good agreement with numerical simulations (see Fig. 5). Moreover, it is possible to compute the consensus time T_N , which for the voter model turns out to be

$$T_N = \frac{N \langle k^{1+\theta} \rangle^2}{2 \sum_k P(k) k^{2(1+\theta)} \rho_k^S(x=1/2)}. \quad (37)$$

A remarkable agreement between this expression (evaluated numerically) and simulations is found even for some cases where HMF theory fails. Notice that no parameter is fitted. Thus, as we can see in Fig. 6, for small values of θ ($\theta = 0.5$) and small γ , both HMF theory and the HPA provide accurate results for the consensus time. Larger values of the weight exponent ($\theta = 1.5$) are well represented by HPA, while HMF fails.

For larger values of θ , however, even the HPA approximation is not sufficient to capture the correct behavior of the model. In this regime, a much harsher breakdown of the HMF assumptions occurs [5,23]: The state of a node of degree k (or of an edge joining vertices of degree k and k') depends not

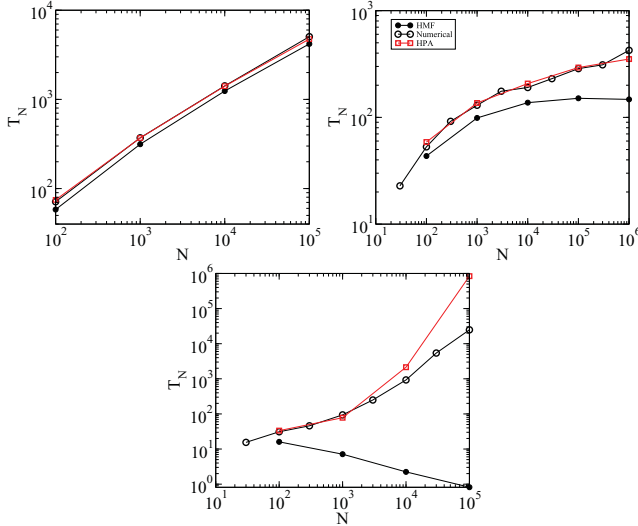


FIG. 6. (Color online) Comparison of the consensus time T_N as a function of N obtained in numerical simulations for voter dynamics on quenched networks (open circles) and the results of the numerical evaluation of the HMF, Eq. (23) (filled circles), and HPA, Eq. (37) (open squares) predictions. Data correspond to networks with $\gamma = 2.75, \theta = 0.5$ (top), $\gamma = 3.25, \theta = 1.5$ (center), and $\gamma = 4, \theta = 4$ (bottom).

only on the degrees but on the detailed quenched structure of the network, much beyond single-node or single-pair features. For example, as $\theta \rightarrow \infty$ [5], each node interacts deterministically with its most connected neighbor. According to HMF equations, which describe an annealed scenario, this means that every node will select the most connected node(s) in the network. However, in a quenched structure each node can choose its partner only among its neighbors, with the result that different portions of the network will effectively become independent from the point of view of the dynamics. Different regions of the network may therefore order in different states, and in this case the final global consensus will never be reached (see also Ref. [5]).

VI. CONCLUSIONS

We have presented a detailed investigation of the behavior of voter model and Moran processes on weighted complex networks. From the analytical point of view we have put forward a theoretical framework that allows to deal with generic edge weights. For a specific form of the weights we have derived in detail all relevant properties of the dynamical processes, such as the exit probability and the scaling of the consensus time as a function of the network size. It turns out that the presence of weights has the effect of slowing down the Moran process with respect to the unweighted case, while it generally speeds up ordering with voter dynamics. Numerical simulations are in good agreement with the theory for small absolute values of θ , while for large $|\theta|$ substantial discrepancies show up. An improved mean-field-like theoretical approach (heterogeneous pair approximation) taking into account two-body correlations gives better agreement with numerics. Still in the limit of large positive (negative) θ , when the state of a node tends to be deterministically enslaved to the state of its neighbor with largest (smallest) degree, the theoretical approaches fail to describe in a satisfactory manner the behavior of the system.

The positive news is that the mean-field equations describe quite well the dynamics observed in real (quenched) networks for weight intensities of the order of the ones observed in real-world networks [1]. However, the generality of this finding, as well as the intrinsic limits of the theory, are in need of a better understanding (see also Ref. [5]). A theoretical approach able to take into account the detailed quenched structure of weighted networks is in order to successfully tackle this problem.

ACKNOWLEDGMENTS

R.P.-S. and A. B. acknowledge financial support from the Spanish MEC (FEDER), under project No. FIS2010-21781-C02-01, and the Junta de Andalucía, under project No. P09-FQM4682. R.P.-S. acknowledges additional support through ICREA Academia, funded by the Generalitat de Catalunya. A.B. acknowledges support of Spanish MCI through the Juan de la Cierva program funded by the European Social Fund.

-
- [1] A. Barrat, M. Barthélemy, R. Pastor-Satorras, and A. Vespignani, *Proc. Natl. Acad. Sci. U.S.A.* **101**, 3747 (2004).
 - [2] M. Barthélemy, A. Barrat, R. Pastor-Satorras, and A. Vespignani, *Physica A* **346**, 34 (2005).
 - [3] A. Barrat, M. Barthélemy, and A. Vespignani, in *Large Scale Structure and Dynamics of Complex Networks: From Information Technology to Finance and Natural Sciences*, edited by G. Caldarelli and A. Vespignani (World Scientific, Singapore, 2007), pp. 67–92.
 - [4] A.-C. Wu, X.-J. Xu, Z.-X. Wu, and Y.-H. Wang, *Chin. Phys. Lett.* **24**, 577 (2007).
 - [5] A. Baronchelli and R. Pastor-Satorras, *Phys. Rev. E* **82**, 011111 (2010).
 - [6] G. Yan, T. Zhou, J. Wang, F. Zhong-Qiang, and W. Bing-Hong, *Chin. Phys. Lett.* **22**, 510 (2005).
 - [7] V. Colizza and A. Vespignani, *Phys. Rev. Lett.* **99**, 148701 (2007).
 - [8] C. V. Giuraniuc, J. P. L. Hatchett, J. O. Indekeu, M. Leone, I. Pérez Castillo, B. Van Schaeybroeck, and C. Vanderzande, *Phys. Rev. Lett.* **95**, 098701 (2005).
 - [9] M. Karsai, R. Juhász, and F. Iglói, *Phys. Rev. E* **73**, 036116 (2006).
 - [10] A. Baronchelli, A. Barrat, and R. Pastor-Satorras, *Phys. Rev. E* **80**, 020102 (2009).
 - [11] C. Castellano, S. Fortunato, and V. Loreto, *Rev. Mod. Phys.* **81**, 591 (2009).
 - [12] P. Clifford and A. Sudbury, *Biometrika* **60**, 581 (1973).
 - [13] R. Holley and T. Liggett, *Ann. Probab.* **3**, 643 (1975).
 - [14] P. Moran, *The Statistical Processes of Evolutionary Theory* (Clarendon, Oxford, U.K., 1962).

- [15] M. A. Nowak, *Evolutionary Dynamics* (Berknep/Harvard, Cambridge, MA, 2006).
- [16] K. Suchecki, V. M. Eguíluz, and M. S. Miguel, *Europhys. Lett.* **69**, 228 (2005).
- [17] C. Castellano, in *Modeling Cooperative Behavior in the Social Sciences*, edited by J. Marro, P. L. Garrido, and M. A. Muñoz, AIP Conf. Proc. No. 779 (AIP, Melville, NY, 2005), p. 114.
- [18] V. Sood and S. Redner, *Phys. Rev. Lett.* **94**, 178701 (2005).
- [19] T. Antal, S. Redner, and V. Sood, *Phys. Rev. Lett.* **96**, 188104 (2006).
- [20] V. Sood, T. Antal, and S. Redner, *Phys. Rev. E* **77**, 041121 (2008).
- [21] E. Lieberman, C. Hauert, and M. A. Nowak, *Nature (London)* **433**, 312 (2005).
- [22] G. J. Baxter, R. A. Blythe, and A. J. McKane, *Phys. Rev. Lett.* **101**, 258701 (2008).
- [23] C. M. Schneider Mizell and L. M. Sander, *J. Stat. Phys.* **136**, 59 (2009).
- [24] H.-X. Yang, Z.-X. Wu, C. Zhou, T. Zhou, and B.-H. Wang, *Phys. Rev. E* **80**, 046108 (2009).
- [25] Y. Lin, H. Yang, Z. Rong, and B. Wang, *Int. J. Mod. Phys. C* **21**, 1011 (2010).
- [26] S. N. Dorogovtsev, A. V. Goltsev, and J. F. F. Mendes, *Rev. Mod. Phys.* **80**, 1275 (2008).
- [27] A. Barrat, M. Barthélemy, and A. Vespignani, *Dynamical Processes on Complex Networks* (Cambridge University Press, Cambridge, UK, 2008).
- [28] E. Pugliese and C. Castellano, *Europhys. Lett.* **88**, 58004 (2009).
- [29] R. Pastor-Satorras, A. Vázquez, and A. Vespignani, *Phys. Rev. Lett.* **87**, 258701 (2001).
- [30] S. N. Dorogovtsev and J. F. F. Mendes, *Evolution of Networks: From Biological Nets to the Internet and WWW* (Oxford University Press, Oxford, UK, 2003).
- [31] C. W. Gardiner, *Handbook of Stochastic Methods*, 2nd ed. (Springer, Berlin, 1985).
- [32] F. Vázquez and C. López, *Phys. Rev. E* **78**, 061127 (2008).
- [33] M. Boguñá and R. Pastor-Satorras, *Phys. Rev. E* **66**, 047104 (2002).
- [34] M. Catanzaro, M. Boguñá, and R. Pastor-Satorras, *Phys. Rev. E* **71**, 027103 (2005).
- [35] M. Boguñá, R. Pastor-Satorras, and A. Vespignani, *Eur. Phys. J. B* **38**, 205 (2004).
- [36] C. Castellano, D. Vilone, and A. Vespignani, *Europhys. Lett.* **63**, 153 (2003).